Ecological Modelling 486 (2023) 110507

Contents lists available at ScienceDirect

Ecological Modelling

journal homepage: www.elsevier.com/locate/ecolmodel

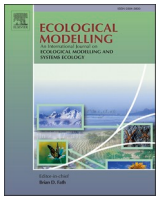

Interactive effects of microbial functional diversity and carbon availability on decomposition – A theoretical exploration

Swamini Khurana [a,b], Rose Abramoff [c,d], Elisa Bruni [e], Marta Dondini [f], Boris Tupek [g], Bertrand Guenet [e], Aleksi Lehtonen [g], Stefano Manzoni [a,b,*]

[a] Department of Physical Geography, Stockholm University, Stockholm SE-106 91, Sweden
[b] Bolin Centre for Climate Research, Stockholm University, Stockholm SE-106 91, Sweden
[c] Climate and Ecosystem Sciences Division, Lawrence Berkeley National Laboratory, Berkeley, CA, USA
[d] Ronin Institute, Montclair, NJ, USA
[e] LG-ENS (Laboratoire de Géologie) CNRS UMR 8538 - Ecole Normale Supérieure, PSL University - IPSL, Paris, France
[f] School of Biological Sciences, University of Aberdeen, 23 St Machar Drive, Aberdeen, Scotland AB24 3UU, UK
[g] Natural Resources Institute Finland, Latokartanonkaari 9, Helsinki FI-00790, Finland

ARTICLE INFO

Keywords:
Microbial model
Organic matter decomposition
Organic carbon oxidation state
Decomposition kinetics
Microbial diversity-function relation
Microbial functional trait

ABSTRACT

Microbial functional diversity in litter and soil has been hypothesized to affect the rate of decomposition of organic matter and other soil ecosystem functions. However, there are no clear theoretical expectations on how these effects might change with substrate availability, heterogeneity in the substrate chemistry, and different aspects of functional diversity itself (number of microbial groups vs. distribution of functional traits). To explore how these factors shape the decomposition-diversity relation, we carry out numerical experiments using a flexible reaction network comprising microbial processes and interactions with bioavailable carbon (extracellular degradation, uptake, respiration, growth, and mortality), and ecological processes (competition among the different groups). We also considered diverse carbon substrates, in terms of varying nominal oxidation state of carbon (NOSC). The reaction network was used to test the effects of (i) number of microbial groups, (ii) number of carbon pools, (iii) microbial functional diversity, and (iv) amount of bioavailable carbon. We found that the decomposition rate constant increases with increasing substrate concentration and heterogeneity, as well as with increasing microbial functional diversity or variance of microbial traits, albeit these biological factors are less important. The multivariate dependence of the decomposition rate constant (and other decomposition and microbial growth metrics) on substrate and microbial factors can be described using power laws with exponents lower than one, indicating that diversity effects on decomposition and microbial growth are reduced at high substrate concentration and heterogeneity, or at high microbial diversity.

1. Introduction

Microbial diversity refers to the range of microbial organisms in a system and is typically measured in terms of taxonomic units or functional groups (Scow et al., 2001). Microbial diversity has been linked to soil organic carbon decomposition and microbial respiration (Setälä and McLean, 2004; Bell et al., 2005; Nielsen et al., 2011; Valentin et al., 2014) and may be one of the determinants for the resilience of soil ecosystems to change in environmental conditions (Snajdr et al., 2010; Valentin et al., 2014; Waring and Hawkes, 2018; Osburn et al., 2021). Zhou et al. (2012) showed that microbial diversity is a key predictor for soil organic carbon respiration using statistical approaches; thus, diversity can have quantitatively important effects. These links between diversity and respiration are due to both the intrinsic decomposition capacity of microbial communities, and the feedbacks between diversity and organic matter stability. In fact, the characteristics of soil organic matter (not only its decomposability) depend on the composition of the microbial community that mediates its formation (Domeignoz-Horta et al., 2021; Sokol et al., 2022). Yet, specific mechanisms to explain these effects are not well understood. Moreover, the structure and composition of microbial communities change in time and space (Lohmann et al., 2020), which adds further complexity to diversity-driven patterns.

To explore the relationship of the microbial diversity and organic

* Corresponding author at: Department of Physical Geography, Stockholm University, Stockholm SE-106 91, Sweden.
E-mail address: stefano.manzoni@natgeo.su.se (S. Manzoni).

https://doi.org/10.1016/j.ecolmodel.2023.110507
Received 17 July 2023; Received in revised form 8 September 2023; Accepted 12 September 2023
Available online 10 October 2023

matter decomposition (and other soil functions), several manipulation studies were carried out at the field and lab scale (Nielsen et al., 2011; Valentin et al., 2014; Vicena et al., 2022). While there is no clear answer on the nature of the diversity-function relations yet, the majority of the studies revealed a positive relationship (e.g., Setälä and McLean 2004; Bell et al. 2005). Consistent with this empirical evidence, theoretical models predict that decomposer diversity should promote decomposition and nutrient recycling (Loreau, 2001). However, how to incorporate microbial diversity metrics in process-based soil carbon models remains an open question.

It is particularly challenging to represent the microbial diversity effect on decomposition because microbially explicit models represent the microbial populations with several, often poorly constrained parameters (Marschmann et al., 2019). Microbial explicit numerical models have been useful to study reactive systems mediated by bacteria, saprotrophic fungi and mycorrhizal fungi, feeding on residues (possibly of different quality) or carbon supplied by plants. Most of these models focused on the interactions of one or few carbon compounds with microbial biomass as a whole (Schimel and Weintraub, 2003; Manzoni and Porporato, 2009; Wieder et al., 2015). A few models break down the microbial community into functional groups at a rather coarse taxonomic or functional level (Li et al., 1992; Grant et al., 1993; Kersebaum and Richter, 1994; Maggi et al., 2008; Kaiser et al., 2014; Baskaran et al., 2017), but the structure of these models does not allow manipulating diversity per se.

Lastly, the above mentioned models were mostly developed for predictive purposes, or for exploration of food web dynamics, and they did not consider microbial (functional) diversity per se and its role in carbon cycling. There are some exceptions, in which functional diversity is manipulated in silico to gain theoretical insights on organic matter dynamics in either a generic ecosystem (Loreau, 2001) or marine systems (Zakem et al., 2021). Studying diversity effects requires modelling a number of microbial groups interacting with a diverse set of carbon compounds and is complicated by the nearly total lack of information on the kinetics regulating decomposition potential, assimilation, growth, and mortality of the individual microbial groups. Not only the mathematical form of the kinetics, but also the parameter values for the kinetics laws are uncertain. Developing a simple approach to represent the effect of microbial diversity on decomposition is therefore needed to help large scale process based model to better represent microbial community composition effects on decomposition and other microbial functions.

To overcome the intrinsic limitation of parametrization, generic parameterizations can be developed based on more or less strict 'rules' linking the parameter values in the prescribed kinetic laws mediating each microbial-substrate interaction. For example, random kinetic parameter values can be prescribed to account for the stochastic nature of microbial communities (Zakem et al., 2021). This allows identifying the intrinsic effects of food web structure (number and diversity of functional groups; how necromass is recycled) on the overall decomposition process and organic carbon accumulation. In addition, physiological trade-offs and coordination between pairs of physiological processes can be accounted for by imposing some degree of correlation (negative for trade-offs, positive for coordinated processes) among the parameter values in the microbial kinetics (Allison, 2012). Competition and facilitation mechanisms also play a role within decomposer communities (Allison, 2005; Kaiser et al., 2014). Accounting for parameter variability and co-variation, and for the basic mechanisms of interaction among functional groups, ensures incorporation of some of the processes responsible for biodiversity effects (Pilowsky et al., 2022).

In this contribution, using a flexible decomposition model including multiple substrates and microbial functional groups, we link ecosystem functions associated with organic matter decomposition to microbial diversity. Specifically, we ask: how do initial microbial community characteristics (in terms of size and functional diversity) affect ecosystem functions such as decomposition rates or microbial growth and functional diversity during decomposition? With our model, we traced the consumption of organic carbon in diverse microbial functional groups whose decomposition capacity and metabolism are controlled by randomly varying and partly co-varying parameters. With this information, we quantify the above-mentioned ecosystem functions and propose a rate modifier to capture the effects of substrate and microbial diversity on decomposition rates.

2. Materials and methods

2.1. Reaction network

The reaction network comprises a number N_c of carbon compounds (denoted by i in Fig. 1, with $3 \leq N_c \leq 18$) that together form the bioavailable substrate carbon pool (C), and a number of microbial functional groups N_b (denoted by j in Fig. 1 with $4 \leq N_b \leq 32$) that together form the microbial biomass pool (B). The minimum N_c and N_b are set to avoid having a network driven by one or two compartments characterized by extreme parameter values (parameter values are randomly sampled, see Section 2.2). The substrate carbon compounds are differentiated based on the nominal oxidation state of the carbon atoms ($NOSC$). The reaction network describes the interactions between pairs i, j of carbon substrates and microbial groups including the depolymerization of carbon compounds ($D_{i,j}$), the uptake of these compounds ($U_{i,j}$) by microbes for growth and assimilation into biomass ($G_{i,j}$), respiration ($R_{i,j}$), and finally necromass (C_B) formation (at a rate M_j) and recycling of necromass into the substrate compartments. The reaction network is illustrated in Fig. 1A; symbols are listed and explained in Table 1.

We tuned the model to describe condition in the top soil, where total carbon concentrations range between 0.2 and 20 mol C kg^{-1} (Xu et al., 2013), corresponding approximately to 0.2 and 20 mol C L^{-1} with a bulk density of 1 kg L^{-1} (equivalent to 1 g cm^{-3}). All carbon compound and microbial group variables are expressed as moles of carbon per liter of soil (mol C L^{-1}) and all fluxes as moles of carbon per liter of soil per day (mol C L^{-1} d^{-1}). For convenience, the numerical values in some of the figures are expressed in m mol units.

The reaction network is constructed in accordance with previous works exploring the role of microbial biomass in organic matter decomposition from conceptual (Schimel and Schaeffer, 2012; Kästner et al., 2021) and modelling perspectives (Schimel and Weintraub, 2003; Manzoni and Porporato, 2009; Wieder et al., 2015). The microbial groups produce exoenzymes as a linear function of their biomass (Schimel and Weintraub, 2003),

$$E_j = v_{enz,j} \times B_j, \tag{1}$$

where E_j is the concentration of exoenzyme produced, B_j is the biomass concentration of the jth microbial group, and $v_{enz,j}$ is a proportionality constant. Eq. (1) is interpreted as the steady state solution for enzyme concentration when enzyme production rate scales linearly with microbial biomass and enzymes are deactivated following first order kinetics. Under these assumptions, production ($\sim B$) and deactivation ($\sim E$) are equal, resulting in the proportionality between the enzyme and biomass concentrations ($E \sim B$) captured by Eq. (1). Given the small mass and the uncertainty in the fate of decayed enzymes, we assume for simplicity that deactivated enzymes are lost from the system. The exoenzyme E_j then depolymerizes the carbon compounds following Michaelis Menten kinetics,

$$D_{i,j} = \frac{v_{max_{i,j}} \times C_i \times E_j}{K_{i,j} + C_i}, \tag{2}$$

where, $D_{i,j}$ is the depolymerization rate of the ith carbon compound by the jth microbial group, C_i is concentration of the ith carbon compound, $K_{i,j}$ is the half saturation constant, and $v_{max,i,j}$ is the maximum velocity constant.

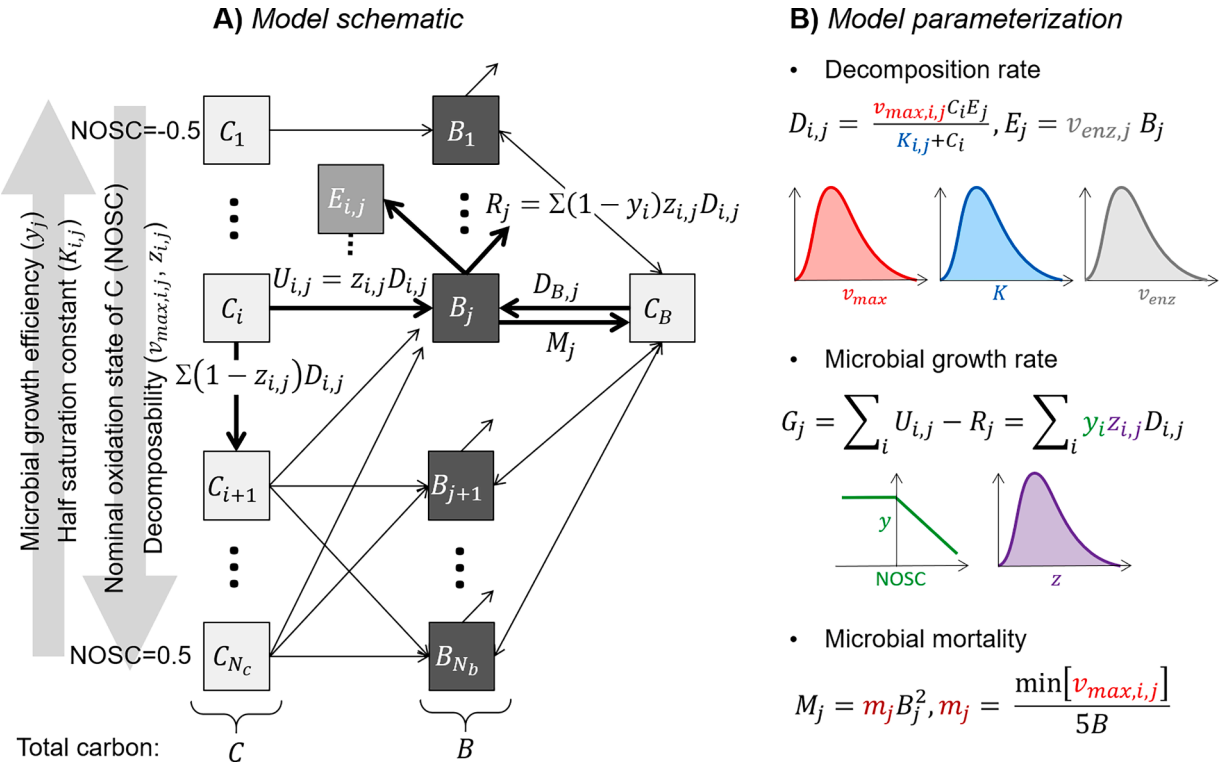

Fig. 1. Schematic representation of the model setup: (A) reaction network and (B) model parameterization, including decomposition, growth, and mortality kinetics and the distributions of their parameters. Microbial necromass is treated as a substrate compartment with NOSC=-0.2 (indicated here by C_B).

Table 1
Symbol definitions and units.

Symbol	Name	Units
Indices and subscripts		
0	Initial conditions (time=0)	-
i	Carbon compound index	-
j	Microbial group index	-
max	At peak biomass or maximum	-
N_c	Number of carbon compounds	-
N_b	Number of microbial groups	-
N_m	Number of carbon compounds that have NOSC=-0.2	-
tot	Total (including substrates and microbial groups)	-
State variables		
B_j	Biomass concentration	mol C L^{-1}
B	Total biomass concentration	mol C L^{-1}
C_i	Substrate organic carbon concentration	mol C L^{-1}
C	Total substrate organic carbon concentration	mol C L^{-1}
C_{tot}	Total organic carbon (= C+B)	mol C L^{-1}
E_j	Exo-enzyme concentration	mol C L^{-1}
Rates		
$D_{i,j}$	Depolymerization	mol C L^{-1} d^{-1}
$U_{i,j}$	Uptake	mol C L^{-1} d^{-1}
$G_{i,j}$	Growth	mol C L^{-1} d^{-1}
M_j	Mortality	mol C L^{-1} d^{-1}
$R_{i,j}$	Respiration	mol C L^{-1} d^{-1}
Parameters		
$f_{reg,j}$	Regulation due to competition	-
$v_{enz,j}$	Proportionality constant	-
$v_{max,i,j}$	Maximum rate of carbon depolymerization	d^{-1}
$v_{prod,i,j}$	Parameter group (= $z_{i,j} \times v_{max_{i,j}} \times v_{enz,j}$)	d^{-1}
$K_{i,j}$	Half saturation constant	mol C L^{-1}
$z_{i,j}$	Uptake efficiency	-
y_i	Growth yield coefficient	-
m_j	Mortality constant	L mol C^{-1} d^{-1}

The depolymerization chain of organic carbon is governed by the nominal oxidation state of the carbon atom (NOSC). The cascade of decomposition of carbon compounds is described in terms of flow of energy (using NOSC as a proxy indicator) following thermodynamic principles (LaRowe and Van Cappellen, 2011; Gunina and Kuzyakov, 2022). Organic matter undergoes change in NOSC as it progresses through decomposition, initially undergoing oxidation and then shifting towards slightly reduced NOSC due to microbial necromass that enters the substrate compartments at an intermediate NOSC level of -0.2 (Kästner et al., 2021; Gunina and Kuzyakov, 2022). Thus, during decomposition, carbon flows to microbial biomass and in part to carbon compounds where carbon has a higher oxidation state. The fraction of carbon compounds that is taken up by microbial biomass is governed by the carbon uptake efficiency of each microbial group,

$$U_{i,j} = z_{i,j} \times D_{i,j}, \quad (3)$$

where, $z_{i,j}$ is the uptake efficiency of each microbial species for each carbon compound. A fraction y_i of the carbon compound taken up is assimilated into the microbial biomass ($G_{i,j}$) and the rest is mineralized into carbon dioxide ($R_{i,j}$). The higher the oxidation state, the lower y_i,

$$G_{i,j} = y_i \times U_{i,j} \times f_{reg,j}, \quad (4)$$

$$R_{i,j} = U_{i,j} - G_{i,j}, \quad (5)$$

where $f_{reg,j}$ is a rate modifier regulating microbial growth due to competition. Based on the previous equations, the growth rate is proportional to the product $v_{prod,i,j}$ of several parameters, $G_{i,j} \sim v_{prod,i,j} = z_{i,j} \times v_{max_{i,j}} \times v_{enz,j}$; this property will be used in Section 2.4 to define microbial functional diversity. Competition due to the presence of other microbial groups followed the Lotka-Volterra model (Vandermeer and Goldberg, 2013; Fujikawa et al., 2014),

$$f_{reg,j} = 1 - \frac{\sum_j (B - B_j)}{B_{max}}, \quad (6)$$

where the carrying capacity of the system (B_{max}) was set to 15 % of initial carbon available for microbial growth. Finally, each microbial group decays due to density-dependent mortality (Georgiou et al., 2017),

$$M_j = m_j B_j^2, \tag{7}$$

where, m_j is the mortality constant of the jth microbial group. The necromass is recycled into the carbon compounds with NOSC=-0.2 (Dick, 2014; Gunina and Kuzyakov, 2022).

Thus, the change in concentration of the ith carbon compound and jth microbial group is given by the coupled mass balances,

$$\frac{dC_i}{dt} = I_i - \sum_j D_{i,j} + \sum_j (1 - z_{i-1,j}) D_{i-1,j} + \begin{cases} \frac{\sum M_j}{N_m}, & NOSC_i = -0.2 \\ 0, & NOSC_i <> -0.2 \end{cases}, \tag{8}$$

$$\frac{dB_j}{dt} = G_j - M_j, \tag{9}$$

where I_i is externally sourced input in the ith carbon compound (in this study, $I_i = 0$) and N_m is the number of carbon compounds that have NOSC =-0.2.

2.2. Parameterization

The parameterization describing the reactions and the state of the carbon compounds was randomized but constrained. The initial oxidation state of the carbon compounds varied between -0.5 and +0.5 (see Fig. 1). We used a slightly higher range of oxidation state of carbon compounds in soil than previously reported (varying between -0.45 and +0.3) (Kleber, 2010) to explore scenarios potentially including aquatic systems.

We randomly sampled the parameters describing microbial-carbon interactions ($v_{enz,j}$, $z_{i,j}$, $v_{max,i,j}$ and $K_{i,j}$) from log normal distributions (Fig. 1, Table 2). The mean values of $v_{max,i,j}$ corresponded with the time scale of decomposition processes, while variation in $z_{i,j}$ represented the capacity of different microbial groups to take up different carbon compounds. The mean of $K_{i,j}$ was chosen to be in the same order of magnitude of bioavailable soil organic carbon concentrations. The variance of these distributions (V_b) changed according to microbial community type (Section 2.3).

The microbial community was also assumed to adapt to available carbon compounds; i.e., $v_{max,i,j}$ is scaled with respect to the initial concentration of the carbon compounds, $C_{i,0}/\overline{C_0}$ (where $C_{i,0}$ is the initial concentration of the i^{th} carbon compound and $\overline{C_0}$ is the mean initial concentration of organic carbon across all substrate compartments).

Carbon compounds with high (positive) NOSC (referred to as oxidized carbon hereon) are easily taken up by microbes for respiration and for complete mineralization, despite their lower energy yield (Gunina and Kuzyakov, 2022). Therefore, we ranked the randomly sampled values of $z_{i,j}$, $v_{max,i,j}$ and $K_{i,j}$ for the various carbon compounds according to the NOSC of each compound. So higher values of $z_{i,j}$ and $v_{max,i,j}$ were associated with higher NOSC while lower values of $K_{i,j}$ were associated with higher NOSC. Finally, y_i for each carbon compound depended on the oxidation state of that compound ($NOSC_i$) (Manzoni et al., 2012b),

$$y_i = \begin{cases} 0.6, & NOSC_i \le 0 \\ 0.6 - \frac{NOSC_i}{3}, & NOSC_i > 0 \end{cases}. \tag{10}$$

Lastly, the mortality constant of each microbial group (m_j) was scaled with the median value of $v_{max,i,j}$ associated with that microbial group and the total initial biomass in the system,

$$m_j = \frac{\underset{i}{\text{median}} v_{max,i,j}}{5 \sum_j B_{j,0}}, \tag{11}$$

where the factor five in the denominator ensured that microbial groups were stable and were able to grow even in carbon poor conditions.

Table 2
Mean values of the log-normal distributions from which decomposition parameters are sampled. The variances of the distributions is assumed proportional to the mean values through a coefficient V_b.

Parameter	Mean	Units
$z_{i,j}$	0.2	-
$v_{max,i,j}$	0.004	d^{-1}
$K_{i,j}$	0.6	mol C L^{-1}
$v_{enz,j}$	0.4	-

2.3. Scenarios

2.3.1. Variation in initial substrate carbon (C_0)

To reflect large variations in the available organic carbon concentration (e.g., across land uses, land covers, soil types), we considered scenarios with a range of initial available organic carbon (C_0) from 1 to 15 mol C L^{-1} (Fig. 2B).

2.3.2. Carbon compounds and microbial groups

Organic matter in natural systems is composed of a spectrum of carbon compounds and their diversity depends on the stage of decomposition and the ecosystem being modeled. We considered diversity in terms of number of compounds making up organic carbon in the system. The number of carbon compounds varied from 3 to 18 (N_c = 3, 6, 12, 18). Thus, for each value of initial organic carbon concentration, the percentage of contribution of each carbon compound varied according to the total number of carbon compounds in the system.

Overall, the initial biomass in all the scenarios was maintained at 10 % of the initial concentration of organic matter. The number of microbial groups also varied (N_b = 4, 8, 12, 16, 20, 24, 28, 32) in each scenario considered for the varying number of carbon compounds.

Combining different numbers of carbon compounds and microbial groups already resulted in a wide variety of initial Shannon diversity indices (H) for each simulation,

$$H = -\sum_j (p_j \log p_j), \tag{12}$$

where, $p_j = \frac{B_j}{\sum_j B_j}$, and B_j is the biomass of the jth microbial functional group. The resulting Shannon diversity varied from less than 1 to greater than 3.

As mentioned in Section 2.2, we also varied the variance (V_b) in the parameter space governing microbial-carbon interactions. We considered five levels of V_b: 1, 10, 50, 100 and 150 % of the mean of the parameter of concern (Table 2). In doing so, we accounted for homogeneous and generalist communities (with low V_b) as well as heterogeneous and specialist communities (with high V_b). Thus, to assess microbial diversity, we explored the utility of both taxonomic diversity (in terms of H, see above) as well as functional diversity (in terms of V_b or f, see below). To have a representative ensemble of simulations in the randomized scenarios, we used nine different seeds to initialize the scenarios. This procedure provided nine replicate simulations for each combination of C_0, N_c, N_b, and V_b.

We simulated all the above-described scenarios for a period of 10 years, using the reaction network set up in Python (van Rossum and Drake, 2006) with the SciPy 1.0 package (Virtanen et al., 2020) as the numerical solver. In total, we ran 800 simulations exploring the rate of carbon consumption in systems with varying total available carbon, number of carbon compounds, number of microbial groups and varying

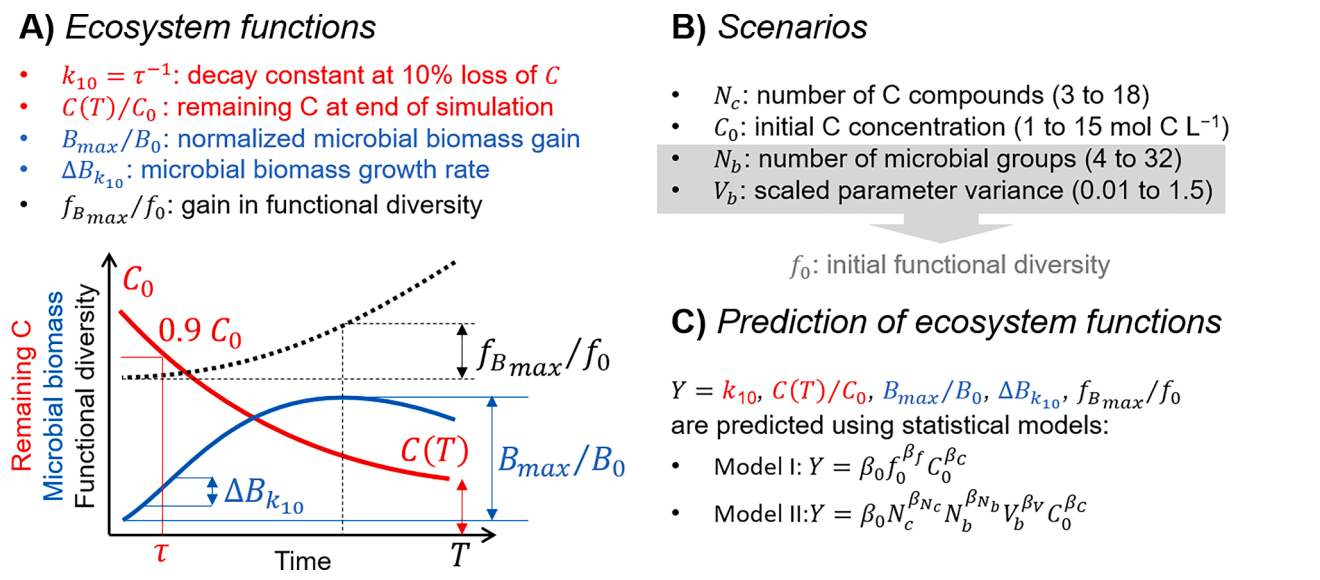

Fig. 2. (A) Summary of ecosystem functions associated with carbon decomposition in the modelled microbial system. (B) Summary of the scenarios for the modelling experiments. (C) Summary of statistical models fitted to ecosystem functions based on the numerical experiments.

microbial community characteristics, and finally randomized seeds. These scenarios are summarized in Fig. 2B.

2.4. Indices characterizing ecosystem functions

To distinguish the microbial communities between 'homogeneous' and 'heterogeneous', we differentiated between communities not only by their size or taxonomic diveristy (N_b or H), but also by their functional diversity (f). We estimated functional diversity using biomass weighted variance and the product ($v_{prod,i,j}$) of $v_{enz,j}$, $z_{i,j}$, and $v_{max,i,j}$ (see Section 2.1):

$$f = \sum_{i,j} \frac{B_j}{\sum_j B_j} \times \left(v_{prod,i,j} - \overline{v_{prod}}\right)^2, \tag{13}$$

where B_j is the biomass associated with a particular microbial functional group. Communities with f<1.E-5 d^{-2} were described as homogeneous communities, while communities with f>1.E-5 d^{-2} were described as heterogeneous communities.

To evaluate the performance of these model microbial systems, we considered four ecosystem functions (generically denoted by Y and summarized in Fig. 2A) focusing on the ability of a microbial system to decompose organic carbon and to grow:

1 Organic carbon decomposition kinetics: we calculated the time scale (τ, d) associated with the first 10 % loss of total organic carbon; i.e., the sum of substrate carbon and biomass concentration (C_{tot}). The decay constant (k_{10}, d^{-1}) associated with corresponding first order kinetics was the reciprocal of τ. We also traced how the decomposition kinetics evolved as the microbial community consumed carbon for respiration and growth.
2 Persistent carbon: C_{tot} stored in the system at the end of the 10 year simulations as a percentage of initial carbon ($C_{tot,T}/C_{tot,\ 0}$).
3 Normalized microbial biomass gain: The ratio of peak biomass during the simulation period and initial biomass ($B_{max}\ /B_0$). A value of 1 indicates that the microbial community did not gain any biomass.
4 Microbial biomass growth rate: The gain in biomass over 30 days during the initial decomposition stage, i.e., when carbon loss was close to 10 % of C_{tot} ($\Delta B_{k_{10}}$, mol C L^{-1} d^{-1}). Different from $B_{max}\ /B_0$, $\Delta B_{k_{10}}$ represents an actual rate of growth at a specific stage of decomposition and regardless of when the peak biomass is attained.
5 Gain in functional diversity: The ratio of functional diversity at peak biomass and initial function diversity ($f_{B_{max}}/f_0$). A value of 1 indicates that the microbial community did not gain in either diversity or biomass (see above).

2.5. Data analysis

We assessed the predictability of the five ecosystem functions (Y) using two different combinations of predictors as follows:

– Model I: Predictors were initial microbial functional diversity (f_0) and initial available carbon (C_0) and β_0, β_f and β_C were the associated parameters of this model,

$$Y = \beta_0 f_0^{\beta_f} C_0^{\beta_C}. \tag{14}$$

– Model II: Predictors were number of carbon compounds (N_c), number of microbial groups (N_b), variance in the parameter distribution of the microbial groups (V_b) and initial available carbon (C_0) and β_0, β_{N_c}, β_{N_b}, β_V and β_C were associated parameters of this model,

$$Y = \beta_0 N_c^{\beta_{N_c}} N_b^{\beta_{N_b}} V_b^{\beta_V} C_0^{\beta_C}. \tag{15}$$

After log-(base 10) transformation, the above models can be written as linear functions of the independent variables,

$$\log(Y) = \log(\beta_0) + \beta_f \log(f_0) + \beta_C \log(C_0) + \epsilon, \tag{16}$$

$$\log(Y) = \log(\beta_0) + \beta_{N_c} \log(N_c) + \beta_{N_b} \log(N_b) + \beta_V \log(V_b) + \beta_C \log(C_0) + \epsilon. \tag{17}$$

where ϵ is the residual error. Therefore, the β coefficients (except for β_0) can be equivalently interpreted as linear coefficients of the linear regression models in Eqs. (16) and (17), or exponents of the power law relations in Eqs. (14) and (15). We obtained the model parameters by linear least square fitting of the decomposition indices using the scipy package (Virtanen et al., 2020). We used R^2 as a measure of ecosystem function predictability.

3. Results

3.1. Initial microbial diversity

We start by analyzing the functional diversity of the initialized microbial communities. Our definition of microbial community based on the number of microbial groups (N_b) and the variance imposed in the parameter space (V_b) led to initialized communities that varied in Shannon diversity (H) as well as in functional diversity (f) (Fig. S1). By construction, f increased with V_b and N_b, but also with increasing N_c, because more substrates imply a larger number of randomly extracted parameters (one set for each substrate-microbial group link, see Fig. 1). This result supports our assumption that f could summarize the combined effects of substrate and microbial diversity, as described by Model I (see Sections 3.3–3.6).

3.2. Decomposition trajectories

In all the scenarios, microbes consumed substrate carbon for growth and respiration, resulting in a monotonic increase for the percentage of carbon consumed, and in most cases a peaked trajectory for the total microbial biomass (select examples in Fig. 3). The gain in microbial biomass, carbon consumed, and the rate of carbon consumption varied across our scenarios (Fig. 3). The largest variation in biomass growth was controlled by the initial carbon concentration, followed by the number of microbial groups and by microbial diversity in terms of parameter variance (Fig. 3A). In carbon-rich systems, biomass growth showed a distinct peak (Fig. 3A) linked to rapid consumption of available carbon (Fig. 3B), while in carbon-poor systems, biomass growth was minimal and decomposition was relatively slow. Relative to the initial carbon concentration, larger microbial diversity implied faster decomposition and faster microbial growth. The number of microbial groups was crucial for sustaining the biomass over time in carbon-poor systems (e.g., net biomass losses were larger at low N_b, see Fig. 3B). In the following sections, we present in more detail how the five ecosystem functions vary across the different scenarios.

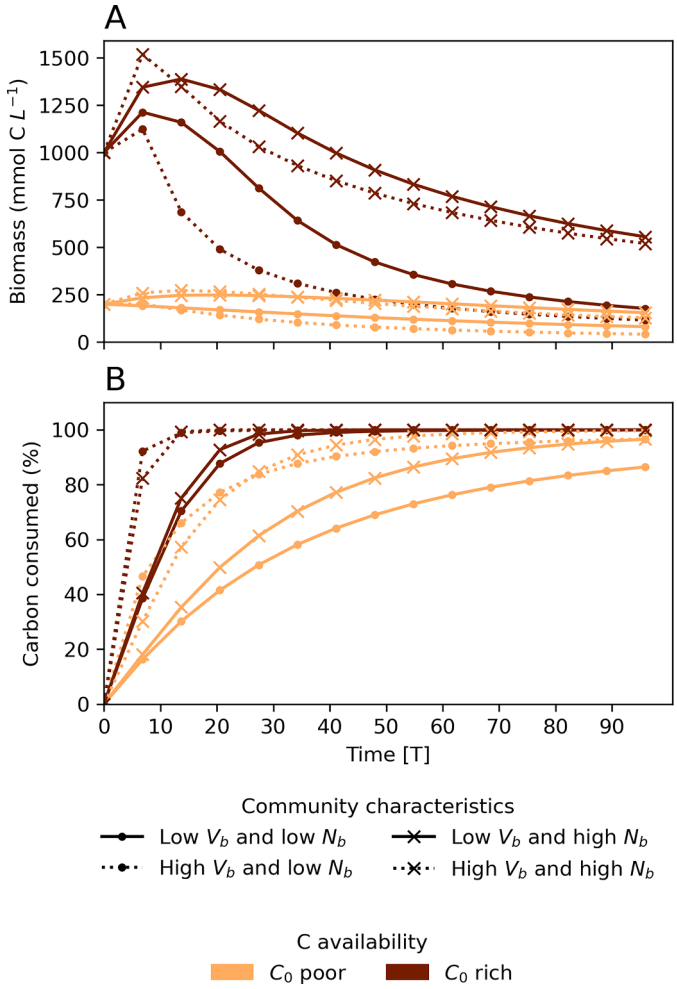

Fig. 3. Temporal trajectories over 10 years of (A) biomass concentration and (B) carbon decomposed (in % with respect to initial available carbon) in selected scenarios. The marker style varies with number of biomass groups: dots for low N_b (4) and cross for high N_b (20). The linestyle varies with microbial community type: solid line for homogeneous communities with low V_b (0.01) and dotted line for heterogeneous communities with high V_b (1.0). The color intensifies with increasing initial carbon concentration from carbon-poor (2 mol C L^{-1}, orange) to carbon rich (10 mol C L^{-1}, brown). The results displayed are for the same randomised scenario, i.e., the seed is the same.

3.3. Decay constant for total organic carbon

Values of k_{10} for C_{tot} varied from 3.2E-4 to 2.0E-1 d^{-1} with a mean of 2.0E-2 d^{-1}, and coefficient of variation ranging from ~20 % (in carbon poor systems with homogeneous communities) to ~50 % (in carbon rich systems). The k_{10} increased significantly with C_0 (Kruskal – Walis test, $p < 0.05$) and with initial microbial diversity f_0 (and H_0, Fig. S2), but the effect of increasing diversity decreased at high diversity levels, as indicated by a coefficient for f_0 lower than one (R^2=0.75 for model I, Fig. 4A). Model II, using the individual predictors of k_{10}, had comparable predictive power as model I (R^2=0.75). All coefficients of both models were positive, indicating that all the considered factors promoted decomposition—especially noteworthy is the positive (priming) effect of initial carbon concentration on decomposition (Fig. 5A, B). Despite reasonable good performance, model I clearly underestimated the sensitivity of k_{10} to changes in f_0 at high carbon availability. Adding an interaction term between f_0 and C_0 in model I did not improve the fitting (results not shown), indicating that model I is structurally inadequate to capture all aspects of diversity effects.

To qualitatively test model results in terms of estimated effects of microbial diversity on decomposition, we compared the coefficients associated with microbial community characteristics in both the models (i.e., β_f, β_{V_b}, and β_{N_b}) to coefficients calculated by fitting power law relations between measured respiration or mass loss and (taxonomic) diversity from published studies (see detailed in Table S1). Model-estimated coefficients lay in the range found from experimental studies, with β_{N_b} at the lower end of the range (Fig. 6).

3.4. Temporal evolution of the decay constant and persistent carbon

The initial carbon concentration affected the decay constant calculated at subsequent steps of 10 % carbon loss. In most scenarios, the decay constant increased (peaking between 80 % and 30 % of C_0 remaining in the system) before decreasing to zero, when decomposition effectively ceased, leaving some persistent, undecomposed carbon in the system (Fig. S3). This unimodal pattern corresponds to a sigmoidal shape in the trajectory of cumulative carbon loss (in the examples in Fig. 3 the initial lagged response of carbon loss is too short to be visible). Both C_0 and the microbial community characteristics (in particular V_b), influenced significantly the temporal evolution of the decay constant (Kruskal Wallis test, $p < 0.05$), with the decay constant increasing more through time with increasing carbon availability and higher diversity in the microbial community.

In carbon poor conditions, decomposition was slow and did not change systematically with subsequent carbon decomposition stages (Fig. S3). The carbon remaining in the system at the end of the simulation period (C_T/C_0 in Fig. 4B) in these conditions was typically 20 % of the initial carbon or higher. Higher initial carbon concentrations and

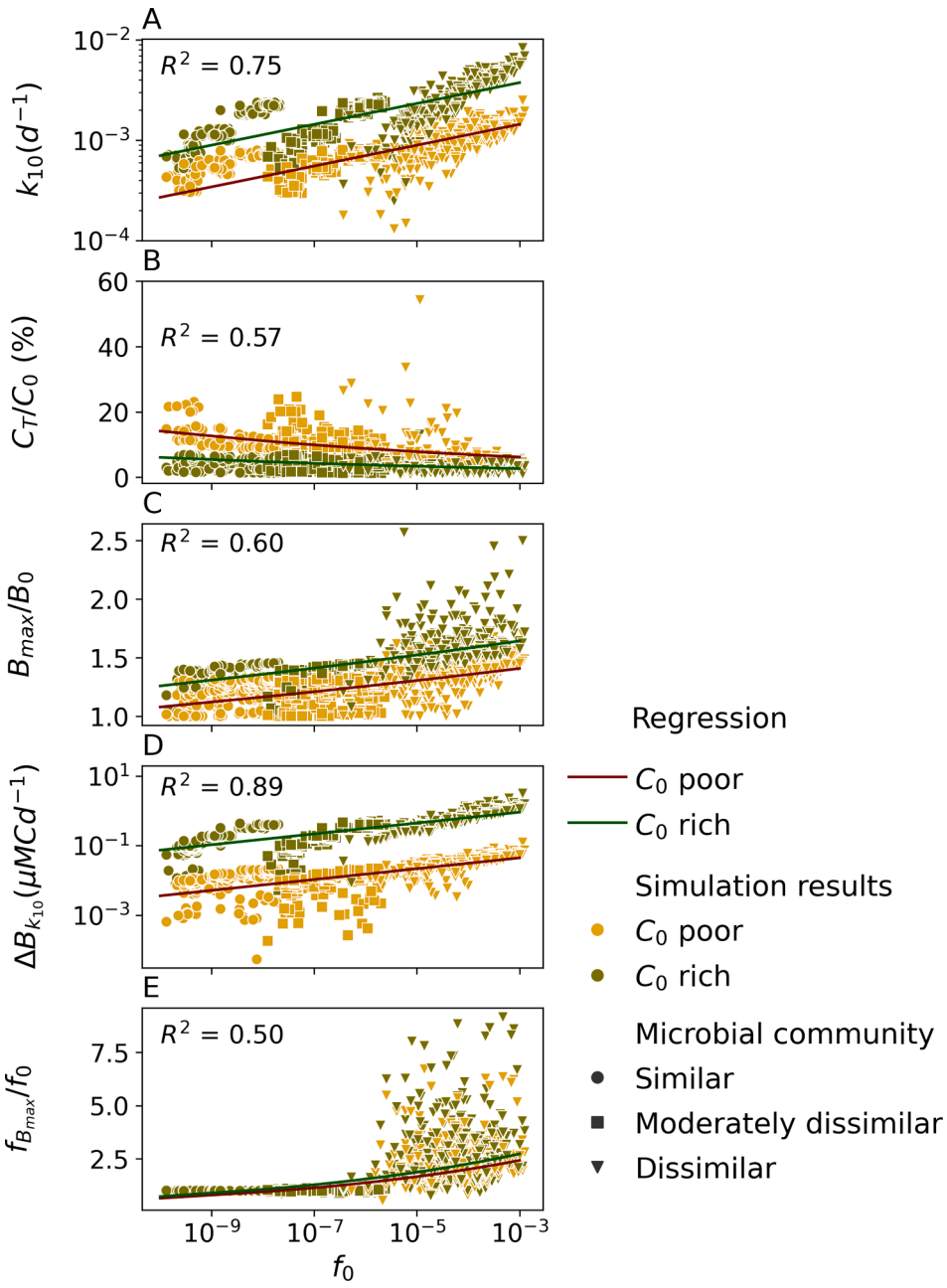

Fig. 4. Ecosystem functions (defined in Fig. 2) in relation to initial functional diversity of microbial communities (f_0, in d^{-2}) and initial carbon concentration (C_0, color coded). To prevent crowding, only selected examples are presented : C_0 = 2 mol C L^{-1} (carbon poor) and C_0 = 10 mol C L^{-1} (carbon rich); V_b=0.01 (homogeneous community) and V_b=1.0 (heterogeneous community): A) initial decay constant (k_{10}) in log scale; B) residual carbon at the end of the simulations (C_T/C_0); C) normalized microbial biomass gain as ratio of maximum biomass and initial biomass (B_{max}/B_0); D) microbial biomass growth rate as gain in biomass over a month at τ_{10} ($\Delta B_{k_{10}}$) in log scale; E) gain in functional diversity ($f_{B_{max}}/f_0$). Regression metrics presented in the panels refer to model I (Eq. (14)) applied to the full dataset, not only the shown data.

higher number of carbon compounds facilitated the decomposition of carbon compounds that would otherwise remain undecomposed (Figs. S4 and S5).

Microbial community characteristics also influenced the persistence of carbon but to a lower extent than initial carbon concentration. Homogeneous communities caused carbon in some compartment to remain undecomposed at the end of the simulation period, while heterogeneous communities contained microbial groups that could decompose otherwise slow-decomposing carbon compounds (e.g., in Fig. S6 microbial necromass carbon cannot be decomposed by a homogeneous community). As a result, the coefficient β_V for C_T/C_0 was negative (Fig. 5B). However, despite the overall positive effect of f_0 on decomposition, in a few systems with highly functionally diverse microbial communities and low initial carbon concentration, C_T/C_0 was as high as 0.6, indicating a disfunctional system (some of the downward triangle orange points in Fig. 4B).

Lastly, a microbial community composed of more functional groups resulted in decomposition of compounds that a community composed of few functional groups could not decompose, but only in systems with low substrate diversity (as in the example in Fig. S7). In general—surprisingly—this was not the case, as shown in the regression analysis, where the coefficient β_{N_b} for C_T/C_0 was relatively large and positive, indicating that communities with more functional groups—all else being equal—were less able to complete the decomposition process

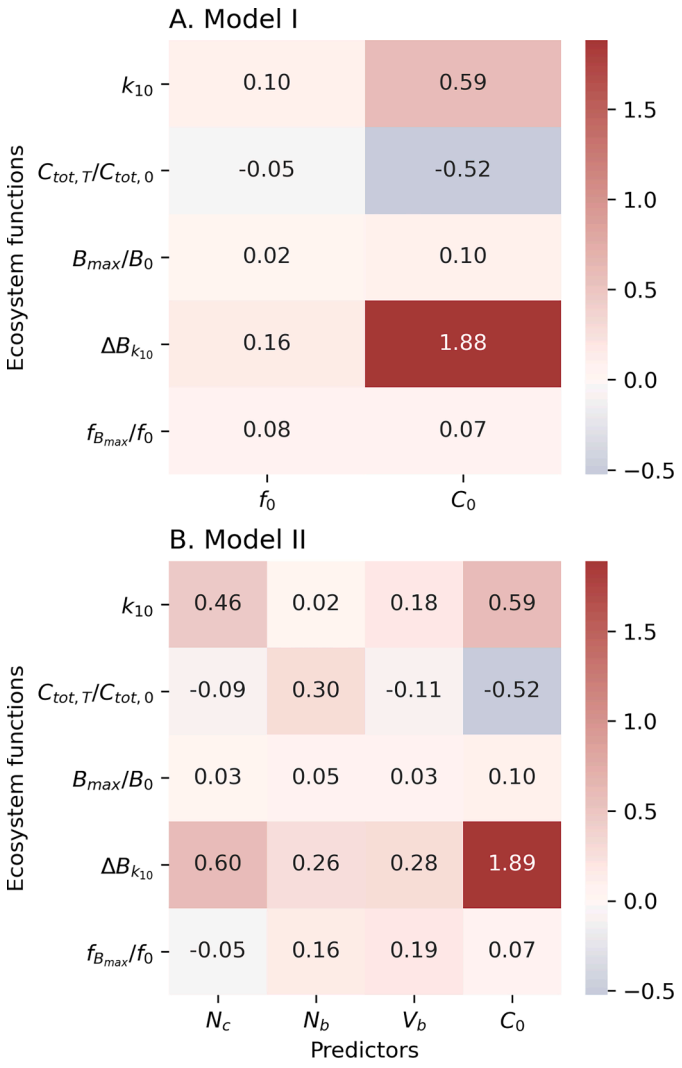

Fig. 5. Coefficients of statistical models predicting ecosystem functions (from top to bottom in each panel: decay constant, persistent carbon, normalized microbial biomass gain, microbial biomass growth rate, change in functional diversity). (A) Model I (Eq. (14)): Coefficients describing the effects of initial functional diversity (f_0) of the community and carbon availability (C_0) on ecosystem functions (coefficients were all different from zero, $p < 0.001$). (B) Model II (Eq. (15)): Coefficients describing the effects of system properties on ecosystem functions: number of carbon compounds (N_c), number of microbial groups (N_b), scaled parameter variance (V_b) and initial carbon concentration (C_0) (coefficients were all different from zero, $p < 0.001$).

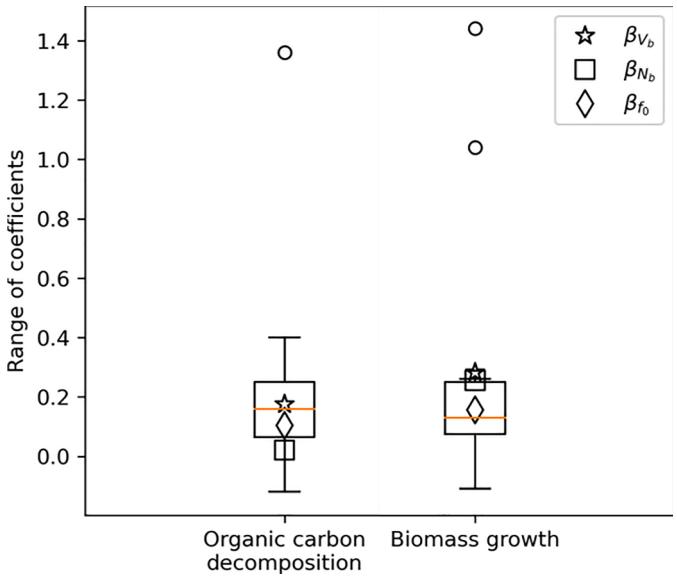

Fig. 6. Comparison of coefficients describing the effect of microbial community characteristics on organic carbon decomposition and biomass growth in our study (i.e., diamond shape for β_f, star shape for β_{V_b}, and square shape for β_{N_b}) with those derived from regression of empirical data, shown as boxplots (median shown in orange and quartiles), with small circles indicating outliers (data from Setälä and McLean 2004; Bell et al. 2005; Tiunov and Scheu 2005; Toljander et al. 2006; Costantini and Rossi 2010; Wilkinson et al. 2012; Valentin et al. 2014; Domeignoz-Horta 2020) (see details in Table S1 for organic carbon decomposition data and in Table S2 for microbial growth data).

than communities with fewer groups (Fig. 5B).

To summarise, the predictability of persistent carbon was moderate ($R^2 = 0.57$). All coefficients for model I were negative, indicating that initial carbon concentration and functional diversity promoted decomposition (mirroring their positive effect on k_{10}) while decreasing the fraction of remaining carbon at the end of the simulations (Fig. 5). In model II, the coefficients of all but one predictor were negative, indicating as in model I that higher initial carbon concentration, number of carbon compounds, and microbial functional diversity (but not the number of microbial groups per se) promoted decomposition (Fig. 5B).

3.5. Microbial biomass gain

Carbon poor systems ($C_0 < 5$ mol C L^{-1}) did not allow for a microbial biomass gain higher than 50 % of initial biomass in most microbial communities. In carbon rich systems, the gain in biomass depended on the nature of the microbial community. Functionally homogeneous communities (low f_0) displayed a lower gain in biomass at its peak (gain of up to 50 % of the initial biomass) compared to heterogeneous communities (peak biomass could be double or more of initial biomass; Fig 4C). Similarly, the microbial biomass growth rate of functionally homogeneous communities was lower than that of heterogeneous communities (Fig. 4D). Extremely heterogeneous communities (functional diversity > 1E-3 d^{-2}) were able to leverage even limited carbon availability to support biomass gains.

The normalized biomass gain could be predicted as a function of f_0 and C_0 (model I) with $R^2 = 0.60$, and the biomass growth rate with $R^2 = 0.89$. The coefficients of this function (i.e., β_f and β_C) were both positive, indicating that both functional diversity and carbon availability promoted biomass growth regarless of how growth is defined (Fig. 5A). Using model II (predictors: N_c, N_b, V_b, and C_0), the normalized biomass gain could be predicted with a comparable $R^2 = 0.61$. The coefficients of this function (i.e., β_{N_c}, β_{N_b}, β_V and β_C) were also positive (but small in magnitude), indicating that number of carbon compounds, microbial diversity (both functional traits and number of groups), as well as initial carbon concentration, promoted biomass growth (Fig. 5B). Similar results were obtained when predicting microbial biomass growth rate, although with stronger effects of all predictors. Moreover, coefficients describing microbial diversity effects on microbial growth were consistent with empirical estimates (Fig. 6).

The initial carbon concentration had a much stronger effect on microbial growth rate compared to the normalized microbial biomass gain (Fig. 5). This difference arised because growth rates were not normalized with respect to the initial states or carbon availability. However, even normalizing growth rates by C_0, coefficients would be slightly lower than one, indicating nearly linear scaling with C_0.

3.6. Microbial community functional diversity

Initially homogeneous communities did not change in functional diversity, while heterogeneous communities became more diverse (Fig. 4E). The transition between these two behaviors occurs at a clear

threshold of $f_0 \approx 10^{-6}$ d^{-2}. The change in functional diversity ($f_{B_{max}}/f_0$) as a function of f_0 and C_0 had $R^2 = 0.50$, while including individual predictors in model II improved the predictability slightly, to $R^2 = 0.53$. All coefficients in both models were positive, except the coefficient for N_c, indicating that a high number of carbon compounds decreased the change of f at peak biomass (Fig. 5B).

4. Discussion

4.1. Model framework rationale and applicability

We set up a reaction network to study how functionally diverse microbial communities degrade organic matter. In this model, functional diversity is driven by the number of microbial groups, number of carbon compounds and the parameter values chosen to represent their decomposition kinetics and metabolism. Communities with higher variance imposed in the parameter distributions can be regarded as composed by diverse microbial functional groups, while communities with low imposed variance are composed by functionally homogeneous and generalist microbial groups. The initial NOSC of the carbon compounds varied between -0.5 and +0.5 but averaged at approximately zero, consistent with bulk soil organic matter in shallow soil, bacterial necromass, litter and some fractions of root exudates (Gunina and Kuzyakov, 2022). With these chemical characteristics and by focusing on only bioavailable chemical compounds, we restrict the interpretation of our results to decomposition of litter or particulate organic carbon, where microbial processes dominate over physical ones (organic matter-mineral interactions are not considered). These systems share similar interactions between microbial decomposers and their substrates. However, the model is not designed to capture the effects of environmental conditions (e.g., soil moisture, temperature, oxygen) on these interactions and these environmental effects can be added for applications to specific systems. Therefore, comparisons of the results in this study can be made with lab scale batch studies where artificial consortia were constructed under prescribed environmental conditions, or natural systems with varying degree of microbial functional diversity due to imposed experimental treatments or natural disturbances, but comparable environmental conditions.

Overall, we observed that the decay constant in all the scenarios varied—mostly decreased—over a multi-year time scale, which was consistent with previous evidence of slowing down of both litter (Manzoni et al., 2012a) and soil organic matter decomposition (Barre et al., 2010). Due to this slowing down, residual organic matter may remain undecomposed or be consumed at negligible rate at the end of our simulation period, similar to observed 'limit values' (Berg et al., 2010). Also the simulated increase in total biomass during decomposition, with subsequent decrease as substrate are depleted, is consistent with observations (van Meeteren et al., 2008) and previous modeling studies (Allison, 2012). Moreover, the model predicts increasing functional diversity as decomposition progresses, which has been observed in e.g., decomposing wood (Valentin et al., 2014). Therefore, at least qualitatively, our reaction network produces dynamics that resemble decomposition in natural systems. A formal calibration is beyond the scope of this work, as we aim to assess the relative differences in ecosystem functions across simulated scenarios, to be compared with studies with manipulated artificial consortia or diversity. However, comparison with previous studies, particularly dilution experiments (Griffiths et al., 2000; Valentin et al., 2014), must also be considered with care as dilution or manipulation may result in some selection bias (Krause et al., 2014).

4.2. Microbial diversity effects: empirical evidence and diversity metrics

Numerous lab and field scale studies have explored the impact on ecosystem functions of microbial diversity expressed as number of species or taxonomic units (Nielsen et al., 2011). Some of these studies showed a positive relationship between microbial diversity and ecosystem functions and others negative (Nielsen et al., 2011; Krause et al., 2014). For example, Liebich et al. (2007) showed using artificial consortia that organic matter mineralization rate was higher in the most diverse community, but the extent of this effect depended on the species present in the consortia and thus their decomposition capacity. The role of functional diversity was particularly important in low microbial diversity consortia, where select combinations of microbial species continued to mineralize at rates comparable to reference complex communities, while other combinations displayed lower mineralization rates, as also observed elsewhere (Setälä and McLean, 2004; Bell et al., 2005; Costantini and Rossi, 2010; Wilkinson et al., 2012; Valentin et al., 2014; Domeignoz-Horta et al., 2020). In another study, diversity increased the organic matter turnover rate (respiration per unit soil carbon), but not the respiration rate per se (Vicena et al., 2022).

In studies where positive correlations between diversity and organic matter loss or respiration were found, also microbial growth increased with diversity (Setälä and McLean, 2004; Costantini and Rossi, 2010; Wilkinson et al., 2012; Domeignoz-Horta et al., 2020) (Tables S1 and S2). In general, facilitation is expected to increase microbial growth and carbon-use efficiency, while competition lowers growth performance (Iven et al., 2023). For example, Toljander et al. (2006) observed that wood decomposition and microbial carbon-use efficiency decreased with increasing number of fungal species (limited to less than 20). This hints at competitive effects among the fungal species in the system, such that some species combinations resulted in slower decomposition. Other experiments showed instead that communities exhibited higher respiration rates, but competition resulted in lower microbial carbon-use efficiency (Maynard et al., 2017)—a process we capture through Eq. (6). Despite the occurrence of negative interactions, our results support the idea that diversity overall promotes microbial growth.

The contrasting diversity effects found in previous studies might in part be caused by the use of taxonomic diversity indices, which is motivating a shift towards functional diversity metrics to understand ecosystem processes (Allison, 2012; Krause et al., 2014). In fact, in these experiments, taxonomic diversity might correlate with functional diversity to a different degree depending on the study, as the selected microbial isolates are not only taxonomically distinct, but also differ in their decomposition capacity. Here, we used biomass weighted variance in functional parameters to characterize microbial communities as homogeneous or heterogeneous (Schleuter et al., 2010). While this metric has been used in plant ecology using measureable functional traits, emerging molecular techniques for microbial activity characterization might provide insights on functional diversity without measuring individual traits in isolates (Cebron et al., 2011; Romillac and Santorufo, 2021).

4.3. Microbial diversity effects: model results

We proceed to discuss the relationships emerging from our model simulations between microbial diversity indicators and ecosystem functions, with a focus on carbon decomposition kinetics. Microbial diversity was positively related with all ecosystem functions except carbon storage (i.e., residual carbon). However, the coefficients of the diversity terms in our regressions were lower than one. These coefficients correspond to exponents of power laws relating functions to diversity, and small exponents imply that the effect of diversity decreases as diversity increases, but without reaching a true saturation level. In other words, in systems with a small microbial community or with low diversity, even a small increase in diversity caused a relatively large change in decomposition capacity, also previously noted experimentally (Setälä and McLean, 2004; Bell et al., 2005; Costantini and Rossi, 2010; Wilkinson et al., 2012; Domeignoz-Horta et al., 2020) and predicted theoretically by Loreau (2001) for generalist communities. In the model by Loreau (2001), the positive effect of species number on ecosystem functions saturates in the communities of generalists,

whereas ecosystem functions continue to benefit from increasing diversity in communities of specialists. Our results suggest a sustained effect of diversity, but with rapidly decreasing effects, indicating that the behavior of our simulated communities is intermediate between generalist and specialist.

The decay constant increased with higher initial carbon concentration, as well as higher substrate and microbial diversity. The increase with carbon availability highlights the importance of nonlinear interactions between microbes and substrates—higher available carbon promotes microbial growth Fig. 4C and D) that in our model feeds-back positively on decomposition—i.e., the model predicts a strong priming effect (Eqs. (1) and ((2)). Thus, in this reaction network, the emerging kinetics are far from linear and predictions from this model differ from linear, microbial-implicit models that do not capture priming effects. Linear models would instead predict that adding carbon will increase the total respiration rate, but will not change the decomposition rate constant. It is also possible that in mineral soils or aquatic systems with low carbon availability (due to physical protection or dilution) these priming effects become less prevalent, lending support for linear approximations.

The coefficients found with our statistical model were comparable to those obtained by fitting respiration or mass loss against microbial taxonomic diversity from previous experimental studies (Setälä and McLean, 2004; Bell et al., 2005; Tiunov and Scheu, 2005; Toljander et al., 2006; Costantini and Rossi, 2010; Wilkinson et al., 2012; Valentin et al., 2014; Domeignoz-Horta et al., 2020), lending support to the overall model setup. Further support—albeit also at a qualitative level—is provided by the comparable values of model-derived and observational coefficients found in microbial growth-diversity relations (Fig. 6).

To apply the derived microbial diversity ecosystem function relationships, information on functional diversity or numbers of microbial groups and carbon compounds should be available, but that information is not readily available—measuring functional diversity is difficult and categorizing microbial groups and carbon compounds might prove impractical or subjective. Therefore, one could consider using the power law model we proposed (in Eqs. (16) and (17)) to describe the relative change in diversity effects induced by a change in diversity. Let us consider the decay constant as an example, which can be expressed by substituting the regression coefficients in Eqs. (16) and (17):

$$k_{10} \propto f_0^{0.10} C_0^{0.59}; \text{ or} \tag{18}$$

$$k_{10} \propto N_c^{0.46} N_b^{0.02} V_b^{0.18} C_0^{0.59}. \tag{19}$$

In a real-case scenario, a measured proxy of microbial functional diversity could indicate a reduction of diversity by half after a disturbance. This would translate into a 10 % reduction in the decay constant all else being equal ($0.5^{0.10} \sim 0.9$, see Fig. 5A). Such scaling arguments could help parameterize diversity effects in soil carbon models (e.g., Abramoff et al. 2022) to improve the predictability of microbe mediated carbon dynamics in soil. The same approach could be used to re-scale the decay constants according to available carbon, as a simple approximation of priming effects.

We are not aware of previous attempts to use power-law relations like Eqs. (18) and (19) to capture the combined microbial and substrate effects on decomposition. While the predictive power of model I Eq. (18)) is not high, and information on the predictors used in model II might not be available, at least some of the scaling arguments proposed here could be applicable as first-order approximations. However, we did not test how varying the mean values of microbial parameters affects the exponents. Thus, to apply these scaling arguments, it would be necessary to first calibrate the mean parameter values and determine site-specific coefficients for Eqs. (18) and ((19).

Not only decomposition or respiration rates, but also microbial growth is promoted by microbial diversity (Fig. 6). For example, a positive effect of taxonomic diversity on growth rates was found by Domeignoz-Horta et al. (2020) in moist soil samples (no effect in dry soil), which was also reflected in a positive effect on microbial carbon-use efficiency. The scaling exponents for the relation between growth rate and number of taxonomic units are slightly above one for this study (with some variation depending on the incubation temperature), indicating a very strong diversity effect. In contrast, our model results suggest exponents ~0.3 for the number of microbial groups and the scaled parameter variance, indicating a weaker diversity effect. This difference might be explained by the shorter time scale of the study by Domeignoz-Horta et al. (2020) (a few months) compared to our multi-year simulations. In our simulations, microbial biomass depends on the balance of growth and mortality, so the signal of diversity might have been smoothed by the long-term growth and decay dynamics in the modelled system. However, the growth-diversity exponents in other studies were more in line with or even lower than our results (Setälä and McLean, 2004; Toljander et al., 2006; Costantini and Rossi, 2010; Wilkinson et al., 2012).

4.4. Functional diversity related thresholds for ecosystem function

We used the biomass weighted variance of the rate constant for decomposition to characterize microbial functional diversity (Schleuter et al., 2010). We then traced the functional diversity of the microbial communities as these communities grew under varying chemical diversity and carbon availability. We found that communities with low functional diversity were likely to die off in carbon poor conditions. This could be attributable to competition for the same resources (Loreau, 2001) because the microbial groups in these communities were similar to each other (low diversity). Due to the lack of niche differentiation in these communities, they were all collectively unable to decompose some carbon compounds, in turn preventing the flow of carbon through the reaction network (Section 3.6). This exacerbated the resource limitation for the communities with low diversity, resulting in their death and incomplete decomposition. In carbon rich conditions, however, this resource limitation was avoided and thus, limited gains in biomass were possible even for these low diversity communities.

In contrast to homogeneous communities, extremely diverse communities grew in biomass and promoted carbon flow through the reaction network even in carbon poor conditions (as also shown by Vicena et al. 2022) thanks to niche differentiation (Loreau, 2001). In carbon rich conditions, these extremely diverse communities grew up to double of their initial biomass. Furthermore, as decomposition progressed, the diversity of these communities also increased (as also shown by Valentin et al. 2014), indicating that microbial groups identified their niches and exploited them ensuring their survival (Allison et al., 2010; Krause et al., 2014). This is in contrast with ecological studies that showed that higher resource supply decreased plant and/or microbial diversity due to enhanced competition (Allison et al., 2010; Krause et al., 2014). Therefore, in the proposed model, mutualism (described as “facilitation effects” by Krause et al. 2014) seems to have outweighed the effects of competition among the microbial groups. In other words, high functional diversity enabled the transfer of carbon among the network compartments, thereby enabling the coexistence of microbial groups. Thus, our results based on a simple model system (for studies including multiple trophic levels, see Dobson et al. 2006; Downing et al. 2012) support the general idea that ecosystems might exhibit thresholds in functional diversity below which they lose functionality.

Furthermore, we observed that diversity of available substrate carbon promoted decomposition (model II). Thus, higher chemical diversity provided microbial groups with more opportunities to occupy their niche, grow, proliferate and consume carbon. This confirmed results from Naeem et al. (2000), who observed that chemical and microbial diversity are positively correlated. In contrast, Loreau (2001) argued that higher chemical diversity resulted in the same or lower recycling efficiency due to inefficiency in resource allocation. Loreau

(2001) did not explore scenarios where $N_c > N_b$, and may have missed testing scenarios where chemical diversity indeed promoted carbon decomposition kinetics. From a more conceptual point of view, it is expected that highly diverse compounds do not promote decomposition because it is not advantageous for microbes to synthesize the specific enzymes needed for all compounds (Lehmann et al., 2020). However, in our model there is no cost in synthesizing enzymes, so that it is not surprising that the positive effect of substrate diversity due to niche differentiation emerges instead of the negative effect due to inefficient carbon economy.

4.5. Methodological limitations

We used the nominal oxidation state of the carbon species to place the substrates in the reaction network and to characterize their decomposability. As a result, NOSC regulates how carbon flows from the 'top' (low NOSC and decomposability) to the 'bottom' (high NOSC and decomposability) of the cascade (Fig. 1), and the growth yield coefficient for each substrate. Instead of this simple approach, we could improve the characterization of the substrates by using Bertz complexity, which uses both molecular weight and the overall compound structure (Cheng et al., 2022). Another alternative would be to assume a continuous change of decomposability, as described by the continuum decay theory (Ågren and Bosatta, 1998) and also used in previous studies (Manzoni and Porporato, 2009).

Regarding processes incorporated in the network, we assumed that exo-enzyme production is upregulated proportionally to the amount of a given carbon species, but we did not penalize microbial groups for costs associated to enzyme production. This means that there is no built-in mechanism in the model to bound the value of $v_{enz,j}$. Similarly, no trade-offs among parameters are considered (except for mortality), so that the parameters describing decomposition ($z_{i,j}$, $v_{\max,i,j}$, $v_{enz,j}$) are treated as independent. This is not necessarily the case, because microbes adopt different strategies involving co-variation of traits to optimize carbon decomposition and biomass growth (Malik et al., 2020). Our reaction network could be parameterized so that microbial compartments match known functional groups (e.g., Allison 2012) with specific set of traits, but this choice would prevent from studying the consequences of varying independently the number of and similarities among microbial groups.

5. Conclusions

We assessed how ecosystem functions, such as decomposition rates and microbial growth, change depending on soil microbial community functional properties and diversity, and with varying carbon availability. To this aim, we formulated a reaction network for microbial processes mediating organic matter decomposition, which was used for theoretical explorations of diversity-function relations. We concluded that carbon availability was a major driver with positive effects on all the ecosystem functions. Furthermore, functional diversity of microbial communities also provided clues as to the overall function of the system. Microbial community diversity (in terms of number of microbial groups and trait variance) promoted ecosystem functions including carbon decomposition and microbial growth, but their effect was reduced at high diversity. Lastly, diversity of substrate carbon also promoted carbon decompositiom as it provided more opportunities for the microbial groups to occupy their niche. Using these results, we suggest that a rate modifier accounting for microbial community characteristics, chemical diversity and carbon availability could be implemented in existing soil carbon models to re-scale the decomposition rate constants depending on the characteristics of the microbial community at a given site.

Declaration of generative AI in scientific writing

During the preparation of this work the authors have not used any generative AI.

CRediT authorship contribution statement

Swamini Khurana: Conceptualization, Methodology, Formal analysis, Data curation, Visualization, Writing – original draft. **Rose Abramoff:** Conceptualization, Methodology, Funding acquisition, Project administration, Writing – review & editing. **Elisa Bruni:** Writing – review & editing. **Marta Dondini:** Writing – review & editing. **Boris Tupek:** Writing – review & editing. **Bertrand Guenet:** Conceptualization, Methodology, Funding acquisition, Project administration, Writing – review & editing. **Aleksi Lehtonen:** Funding acquisition, Project administration, Writing – review & editing. **Stefano Manzoni:** Conceptualization, Methodology, Funding acquisition, Project administration, Visualization, Supervision, Writing – original draft, Writing – review & editing.

Declaration of Competing Interest

The authors declare no competing interests.

Data availability

The model codes are available at: https://doi.org/10.5281/zenodo.8364682.

Acknowledgments

We thank Prof. Alexei Tiunov for sharing microbial respiration data from Tiunov and Scheu (2005) and Dr. Arjun Chakrawal for discussions on organic matter quality. This work was supported by the grant "Holistic management practices, modelling and monitoring for European forest soils" (H2020 grant agreement 101000289). SM has also received funding from the European Research Council (ERC) under the European Union's Horizon 2020 Research and Innovation Programme (SMILE, grant agreement 101001608). RA received funding from Lawrence Berkeley National Laboratory (LBNL), which is managed and operated by the University of California (UC) under U.S. Department of Energy Contract No. DE-AC02-05CH11231.

Supplementary materials

Supplementary material associated with this article can be found, in the online version, at doi:10.1016/j.ecolmodel.2023.110507.

References

Abramoff, R.Z., Guenet, B., Zhang, H., Georgiou, K., Xu, X., Viscarra Rossel, R.A., Yuan, W., Ciais, P., 2022. Improved global-scale predictions of soil carbon stocks with millennial version 2. Soil Biol. Biochem. 164, 108466 https://doi.org/10.1016/j.soilbio.2021.108466.

Ågren, G.I., Bosatta, E., 1998. Theoretical Ecosystem Ecology. Understanding Element Cycles. Cambridge University Press, Cambridge, United Kingdom.

Allison, S.D., 2012. A trait-based approach for modelling microbial litter decomposition. Ecol. Lett. 15, 1058–1070. https://doi.org/10.1111/j.1461-0248.2012.01807.x.

Allison, S.D., 2005. Cheaters, diffusion and nutrients constrain decomposition by microbial enzymes in spatially structured environments. Ecol. Lett. 8, 626–635.

Allison, S.D., Wallenstein, M.D., Bradford, M.A., 2010. Soil-carbon response to warming dependent on microbial physiology. Nat. Geosci. 3, 336–340.

Barre, P., Eglin, T., Christensen, B., Ciais, P., Houot, S., Katterer, T., van Oort, F., Peylin, P., Poulton, P., Romanenkov, V., Chenu, C., 2010. Quantifying and isolating stable soil organic carbon using long-term bare fallow experiments. Biogeosciences 7, 3839–3850. https://doi.org/10.5194/bg-7-3839-2010.

Baskaran, P., Hyvonen, R., Berglund, S.L., Clemmensen, K.E., Agren, G.I., Lindahl, B.D., Manzoni, S., 2017. Modelling the influence of ectomycorrhizal decomposition on plant nutrition and soil carbon sequestration in boreal forest ecosystems. New Phytol. 213, 1452–1465. https://doi.org/10.1111/nph.14213.

Bell, T., Newman, J., Silverman, B., Turner, S., Lilley, A., 2005. The contribution of species richness and composition to bacterial services. Nature 436, 1157–1160. https://doi.org/10.1038/nature03891.

Berg, B., Davey, M.P., De Marco, A., Emmett, B., Faituri, M., Hobbie, S.E., Johansson, M. B., Liu, C., McClaugherty, C., Norell, L., Rutigliano, F.A., Vesterdal, L., De Santo, A. V., 2010. Factors influencing limit values for pine needle litter decomposition: a synthesis for boreal and temperate pine forest systems. Biogeochemistry 100, 57–73.
Cebron, A., Cortet, J., Criquet, S., Biaz, A., Calvert, V., Caupert, C., Pernin, C., Leyval, C., 2011. Biological functioning of PAH-polluted and thermal desorption-treated soils assessed by fauna and microbial bioindicators. Res. Microbiol. 162, 896–907. https://doi.org/10.1016/j.resmic.2011.02.011.
Cheng, W., Hsieh, C., Chang, C., Shiah, F., Miki, T., 2022. New index of functional specificity to predict the redundancy of ecosystem functions in microbial communities. FEMS Microbiol. Ecol. 98 https://doi.org/10.1093/femsec/fiac058.
Costantini, M.L., Rossi, L., 2010. Species diversity and decomposition in laboratory aquatic systems: the role of species interactions. Freshw. Biol. 55, 2281–2295. https://doi.org/10.1111/j.1365-2427.2010.02433.x.
Dick, J., 2014. Average oxidation state of carbon in proteins. J. R. Soc. Interface 11. https://doi.org/10.1098/rsif.2013.1095.
Dobson, A., Lodge, D., Alder, J., Cumming, G., Keymer, J., McGlade, J., Mooney, H., Rusak, J., Sala, O., Wolters, V., Wall, D., Winfree, R., Xenopoulos, M., 2006. Habitat loss, trophic collapse, and the decline of ecosystem services. Ecology 87, 1915–1924. https://doi.org/10.1890/0012-9658(2006)87[1915:HLTCAT]2.0.CO;2.
Domeignoz-Horta, L.A., 2020. Microbial diversity drives carbon use efficiency in a model soil. doi:10.17605/OSF.IO/QMF8Z.
Domeignoz-Horta, L.A., Pold, G., Liu, X.J.A., Frey, S.D., Melillo, J.M., DeAngelis, K.M., 2020. Microbial diversity drives carbon use efficiency in a model soil. Nat. Commun. 11 https://doi.org/10.1038/s41467-020-17502-z.
Domeignoz-Horta, L.A., Shinfuku, M., Junier, P., Poirier, S., Verrecchia, E., Sebag, D., DeAngelis, K.M., 2021. Direct evidence for the role of microbial community composition in the formation of soil organic matter composition and persistence. ISME Commun. 1, 64. https://doi.org/10.1038/s43705-021-00071-7.
Downing, A., van Nes, E., Mooij, W., Scheffer, M., 2012. The resilience and resistance of an ecosystem to a collapse of diversity. PLoS One 7. https://doi.org/10.1371/journal.pone.0046135.
Fujikawa, H., Munakata, K., Sakha, M., 2014. Development of a competition model for microbial growth in mixed culture. Biocontrol Sci. 19, 61–71. https://doi.org/10.4265/bio.19.61.
Georgiou, K., Abramoff, R.Z., Harte, J., Riley, W.J., Torn, M.S., 2017. Microbial community-level regulation explains soil carbon responses to long-term litter manipulations. Nat. Commun. 8, 1223. https://doi.org/10.1038/s41467-017-01116-z.
Grant, R.F., Juma, N.G., McGill, W.B., 1993. Simulation of carbon and nitrogen transformations in soil - mineralization. Soil Biol. Biochem. 25, 1317–1329.
Griffiths, B., Ritz, K., Bardgett, R., Cook, R., Christensen, S., Ekelund, F., Sorensen, S., Baath, E., Bloem, J., de Ruiter, P., Dolfing, J., Nicolardot, B., 2000. Ecosystem response of pasture soil communities to fumigation-induced microbial diversity reductions: an examination of the biodiversity-ecosystem function relationship. OIKOS 90, 279–294. https://doi.org/10.1034/j.1600-0706.2000.900208.x.
Gunina, A., Kuzyakov, Y., 2022. From energy to (soil organic) matter. Glob. Chang. Biol. 28, 2169–2182. https://doi.org/10.1111/gcb.16071.
Iven, H., Walker, T., Anthony, M., 2023. Biotic interactions in soil are underestimated drivers of microbial carbon use efficiency. Curr. Microbiol. 80 https://doi.org/10.1007/s00284-022-02979-2.
Kaiser, C., Franklin, O., Dieckmann, U., Richter, A., 2014. Microbial community dynamics alleviate stoichiometric constraints during litter decay. Ecol. Lett. 17, 680–690. https://doi.org/10.1111/ele.12269.
Kästner, M., Miltner, A., Thiele-Bruhn, S., Liang, C., 2021. Microbial necromass in soils-linking microbes to soil processes and carbon turnover. Front. Environ. Sci. 9 https://doi.org/10.3389/fenvs.2021.756378.
Kersebaum, K.C., Richter, O., 1994. A model approach to simulate C and N transformations through microbial biomass. Eur. J. Agron. 3, 355–360.
Kleber, M., 2010. What is recalcitrant soil organic matter? Environ. Chem. 7, 320–332.
Krause, S., Le Roux, X., Niklaus, P.A., Van Bodegom, P.M., Lennon, J.T., Bertilsson, S., Grossart, H.P., Philippot, L., Bodelier, P.L.E., 2014. Trait-based approaches for understanding microbial biodiversity and ecosystem functioning. Front. Microbiol. 5 https://doi.org/10.3389/fmicb.2014.00251.
LaRowe, D.E., Van Cappellen, P., 2011. Degradation of natural organic matter: a thermodynamic analysis. Geochim. Cosmochim. Acta 75, 2030–2042. https://doi.org/10.1016/j.gca.2011.01.020.
Li, C.S., Frolking, S., Frolking, T.A., 1992. A model of nitrous-oxide evolution from soil driven by rainfall events .1. Model structure and sensitivity. J. Geophys. Res. Atmos. 97, 9759–9776.
Liebich, J., Schloter, M., Schaffer, A., Vereecken, H., Burauel, P., 2007. Degradation and humification of maize straw in soil microcosms inoculated with simple and complex microbial communities. Eur. J. Soil Sci. 58, 141–151. https://doi.org/10.1111/j.1365-2389.2006.00816.x.
Lohmann, P., Benk, S., Gleixner, G., Potthast, K., Michalzik, B., Jehmlich, N., Bergen, M. V., 2020. Seasonal patterns of dominant microbes involved in central nutrient cycles in the subsurface. Microorganisms 8, 1694. https://doi.org/10.3390/microorganisms8111694.
Loreau, M., 2001. Microbial diversity, producer-decomposer interactions and ecosystem processes: a theoretical model. Proc. R. Soc. Lond. Ser. B Biol. Sci. 268, 303–309.
Maggi, F., Gu, C., Riley, W.J., Hornberger, G.M., Venterea, R.T., Xu, T., Spycher, N., Steefel, C., Miller, N.L., Oldenburg, C.M., 2008. A mechanistic treatment of the dominant soil nitrogen cycling processes: model development, testing, and application. J. Geophys. Res. Biogeosci. 113.
Malik, A.A., Martiny, J.B.H., Brodie, E.L., Martiny, A.C., Treseder, K.K., Allison, S.D., 2020. Defining trait-based microbial strategies with consequences for soil carbon cycling under climate change. ISME J. 14, 1–9. https://doi.org/10.1038/s41396-019-0510-0.
Manzoni, S., Pineiro, G., Jackson, R.B., Jobbagy, E.G., Kim, J.H., Porporato, A., 2012a. Analytical models of soil and litter decomposition: solutions for mass loss and time-dependent decay rates. Soil Biol. Biochem. 50, 66–76. https://doi.org/10.1016/j.soilbio.2012.02.029.
Manzoni, S., Porporato, A., 2009. Soil carbon and nitrogen mineralization: theory and models across scales. Soil Biol. Biochem. 41, 1355–1379.
Manzoni, S., Taylor, P.G., Richter, A., Porporato, A., Ågren, G.I., 2012b. Environmental and stoichiometric controls on microbial carbon-use efficiency in soils. New Phytol. 196, 79–91. https://doi.org/10.1111/j.1469-8137.2012.04225.x.
Marschmann, G.L., Pagel, H., Kuegler, P., Streck, T., 2019. Equifinality, sloppiness, and emergent structures of mechanistic soil biogeochemical models. Environ. Model. Softw. 122, 104518 https://doi.org/10.1016/j.envsoft.2019.104518. UNSP.
Maynard, D.S., Crowther, T.W., Bradford, M.A., 2017. Fungal interactions reduce carbon use efficiency. Ecol. Lett. 20, 1034–1042. https://doi.org/10.1111/ele.12801.
Naeem, S., Hahn, D.R., Schuurman, G., 2000. Producer–decomposer co-dependency influences biodiversity effects. Nature 403, 762–764. https://doi.org/10.1038/35001568.
Nielsen, U.N., Ayres, E., Wall, D.H., Bardgett, R.D., 2011. Soil biodiversity and carbon cycling: a review and synthesis of studies examining diversity–function relationships. Eur. J. Soil Sci. 62, 105–116. https://doi.org/10.1111/j.1365-2389.2010.01314.x.
Osburn, E., Badgley, B., Strahm, B., Aylward, F., Barrett, J., 2021. Emergent properties of microbial communities drive accelerated biogeochemical cycling in disturbed temperate forests. Ecology 102. https://doi.org/10.1002/ecy.3553.
Pilowsky, J., Colwell, R., Rahbek, C., Fordham, D., 2022. Process-explicit models reveal the structure and dynamics of biodiversity patterns. Sci. Adv. 8, eabj2271. https://doi.org/10.1126/sciadv.abj2271.
Romillac, N., Santorufo, L., 2021. Transferring concepts from plant to microbial ecology: a framework proposal to identify relevant bacterial functional traits. Soil Biol. Biochem. 162, 108415 https://doi.org/10.1016/j.soilbio.2021.108415.
Schimel, J., Schaeffer, S.M., 2012. Microbial control over carbon cycling in soil. Front. Microbiol. 3 https://doi.org/10.3389/fmicb.2012.00348.
Schimel, J.P., Weintraub, M.N., 2003. The implications of exoenzyme activity on microbial carbon and nitrogen limitation in soil: a theoretical model. Soil Biol. Biochem. 35, 549–563.
Schleuter, D., Daufresne, M., Massol, F., Argillier, C., 2010. A user's guide to functional diversity indices. Ecol. Monogr. 80, 469–484. https://doi.org/10.1890/08-2225.1.
Scow, K.M., Schwartz, E., Johnson, M.J., Macalady, J.L., 2001. Microbial biodiversity, measurement of. Levin, S.A. Encyclopedia of Biodiversity, (2nd ed.). Academic Press, Waltham, pp. 259–270. https://doi.org/10.1016/B978-0-12-384719-5.00434-2.
Setälä, H., McLean, M., 2004. Decomposition rate of organic substrates in relation to the species diversity of soil saprophytic fungi. Oecologia 139, 98–107. https://doi.org/10.1007/s00442-003-1478-y.
Snajdr, J., Steffen, K., Hofrichter, M., Baldrian, P., 2010. Transformation of C-14-labelled lignin and humic substances in forest soil by the saprobic basidiomycetes Gymnopus erythropus and Hypholoma fasciculare. Soil Biol. Biochem. 42, 1541–1548. https://doi.org/10.1016/j.soilbio.2010.05.023.
Sokol, N.W., Slessarev, E., Marschmann, G.L., Nicolas, A., Blazewicz, S.J., Brodie, E.L., Firestone, M.K., Foley, M.M., Hestrin, R., Hungate, B.A., Koch, B.J., Stone, B.W., Sullivan, M.B., Zablocki, O., Pett-Ridge, J., 2022. Life and death in the soil microbiome: how ecological processes influence biogeochemistry. Nat. Rev. Microbiol. https://doi.org/10.1038/s41579-022-00695-z.
Tiunov, A., Scheu, S., 2005. Facilitative interactions rather than resource partitioning drive diversity-functioning relationships in laboratory fungal communities. Ecol. Lett. 8, 618–625. https://doi.org/10.1111/j.1461-0248.2005.00757.x.
Toljander, Y.K., Lindahl, B.D., Holmer, L., Hogberg, N.O.S., 2006. Environmental fluctuations facilitate species co-existence and increase decomposition in communities of wood decay fungi. Oecologia 148, 625–631. https://doi.org/10.1007/s00442-006-0406-3.
Valentin, L., Rajala, T., Peltoniemi, M., Heinonsalo, J., Pennanen, T., Makipaa, R., 2014. Loss of diversity in wood-inhabiting fungal communities affects decomposition activity in Norway spruce wood. Front. Microbiol. 5 https://doi.org/10.3389/fmicb.2014.00230.
van Meeteren, M.M., Tietema, A., van Loon, E.E., Verstraten, J.M., 2008. Microbial dynamics and litter decomposition under a changed climate in a Dutch heathland. Appl. Soil Ecol. 38, 119–127.
van Rossum, G., Drake, F.L., 2006. The Python Language Reference Manual (Version 3.2). Network Theory Ltd.
Vandermeer, J.H., Goldberg, D.E., 2013. Population Ecology: First Principles. Princeton University Press.
Vicena, J., Ardestani, M.M., Baldrian, P., Frouz, J., 2022. The effect of microbial diversity and biomass on microbial respiration in two soils along the soil chronosequence. Microorganisms 10. https://doi.org/10.3390/microorganisms10101920.
Virtanen, P., Gommers, R., Oliphant, T.E., Haberland, M., Reddy, T., Cournapeau, D., Burovski, E., Peterson, P., Weckesser, W., Bright, J., van der Walt, S.J., Brett, M., Wilson, J., Millman, K.J., Mayorov, N., Nelson, A.R.J., Jones, E., Kern, R., Larson, E., Carey, C.J., Polat, İ., Feng, Y., Moore, E.W., VanderPlas, J., Laxalde, D., Perktold, J., Cimrman, R., Henriksen, I., Quintero, E.A., Harris, C.R., Archibald, A.M., Ribeiro, A. H., Pedregosa, F., van Mulbregt, P., SciPy 1. 0 Contributors, 2020. SciPy 1.0: fundamental algorithms for scientific computing in python. Nat. Methods 17, 261–272. https://doi.org/10.1038/s41592-019-0686-2.
Waring, B., Hawkes, C., 2018. Ecological mechanisms underlying soil bacterial responses to rainfall along a steep natural precipitation gradient. FEMS Microbiol. Ecol. 94 https://doi.org/10.1093/femsec/fiy001.

Wieder, W.R., Allison, S.D., Davidson, E.A., Georgiou, K., Hararuk, O., He, Y., Hopkins, F., Luo, Y., Smith, M.J., Sulman, B., Todd-Brown, K., Wang, Y.P., Xia, J., Xu, X., 2015. Explicitly representing soil microbial processes in Earth system models. Glob. Biogeochem. Cycles 29, 1782–1800. https://doi.org/10.1002/2015gb005188.

Wilkinson, A., Solan, M., Alexander, I., Johnson, D., 2012. Species richness and nitrogen supply regulate the productivity and respiration of ectomycorrhizal fungi in pure culture. Fungal Ecol. 5, 211–222. https://doi.org/10.1016/j.funeco.2011.08.007.

Xu, X., Thornton, P.E., Post, W.M., 2013. A global analysis of soil microbial biomass carbon, nitrogen and phosphorus in terrestrial ecosystems. Glob. Ecol. Biogeogr. 22, 737–749. https://doi.org/10.1111/geb.12029.

Zakem, E.J., Cael, B.B., Levine, N.M., 2021. A unified theory for organic matter accumulation. Proc. Natl. Acad. Sci. 118, e2016896118 https://doi.org/10.1073/pnas.2016896118.

Zhou, Y., Kellermann, C., Griebler, C., 2012. Spatio-temporal patterns of microbial communities in a hydrologically dynamic pristine aquifer. FEMS Microbiol. Ecol. 81, 230–242. https://doi.org/10.1111/j.1574-6941.2012.01371.x.